

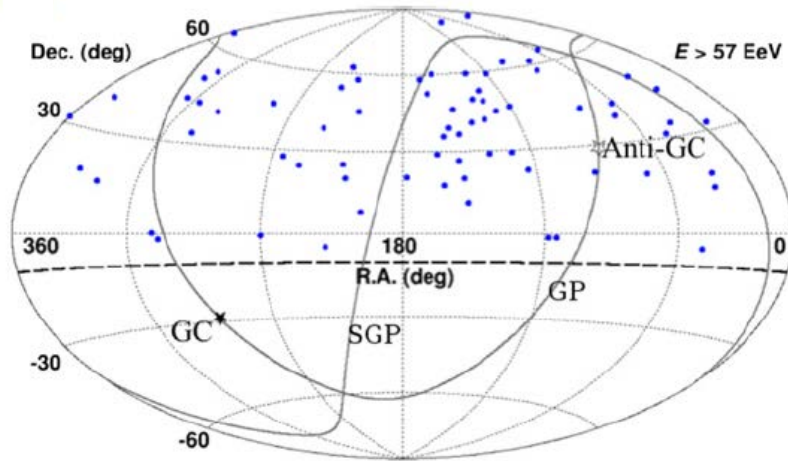
A Close Correlation between TA Hotspot UHECR Events and Local Filaments of Galaxies and its Implication

Jihyun Kim* (Osaka City University),
Dongsu Ryu (UNIST), Hyesung Kang (PNU),
Suk Kim (KASI), Soo-Chang Rey (CNU)

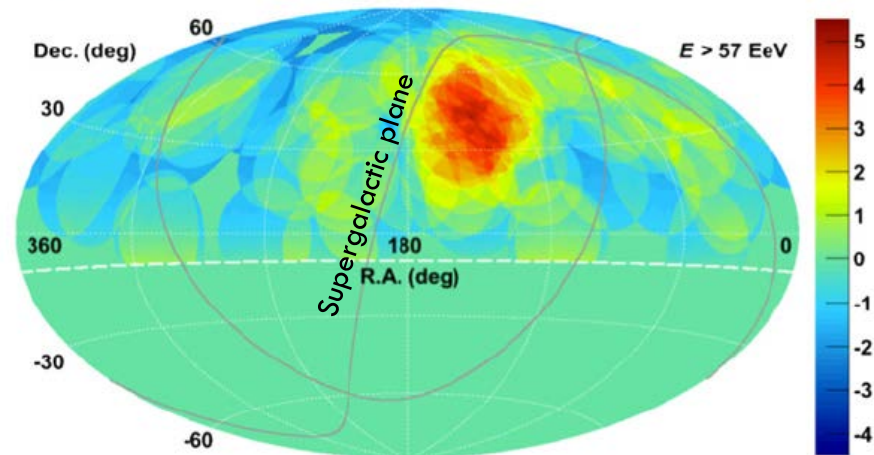
2018-10-10
UHECR 2018 @ Paris

A clustering of TA events TA (2014)

TA events with $E > 5.7 \times 10^{19}$ eV



20° oversampling significance map



Skymaps in the equatorial coordinates

- 72 events with $E > 5.7 \times 10^{19}$ eV (5-year TA SD data)

- Maximum local significance: 5.1σ

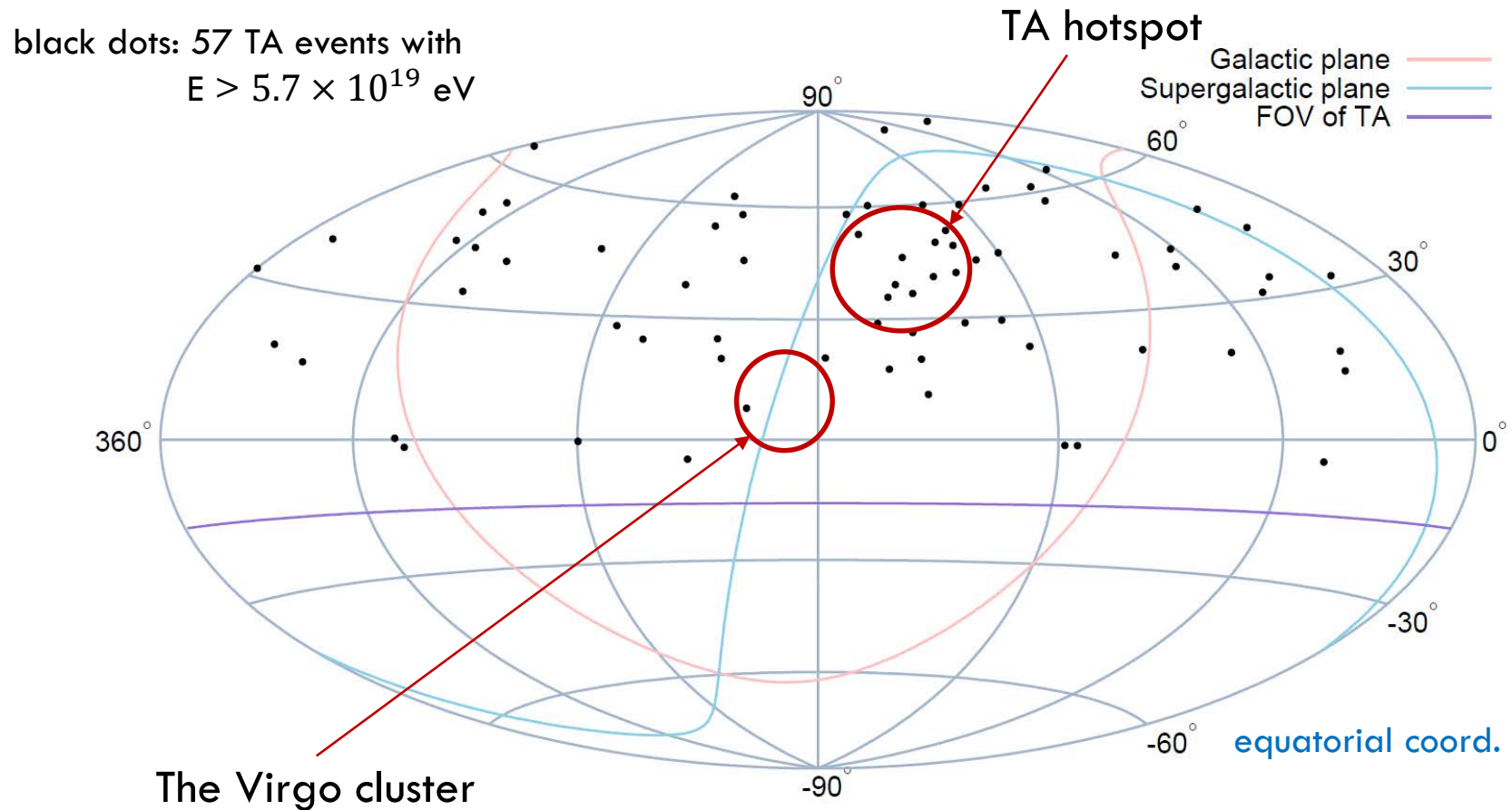
Observed: 19 events

Expected from isotropy: 4.5 events

} $\sim 320\%$ excess to the isotropy

- Post-trial probability: $P(p_{\text{pre}} > 5.1\sigma) = 3.4\sigma$

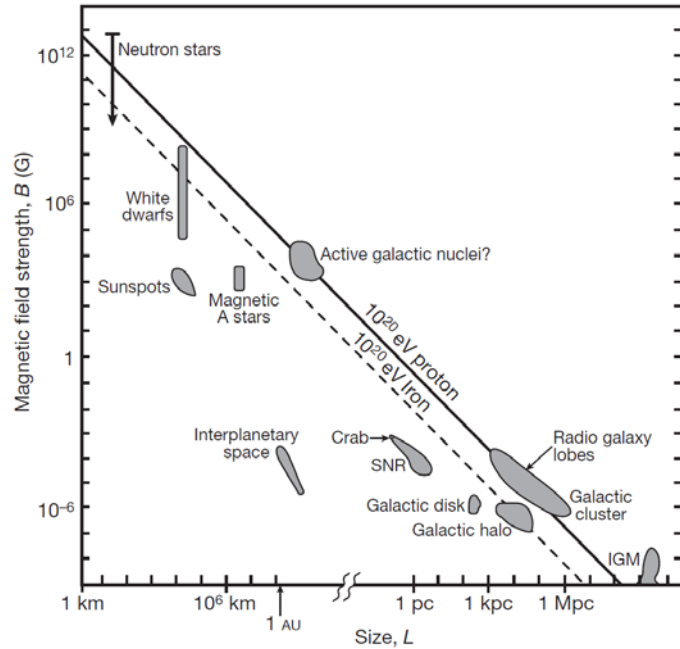
Characteristic distribution of TA events



→ the nature and origin of TA hotspot?

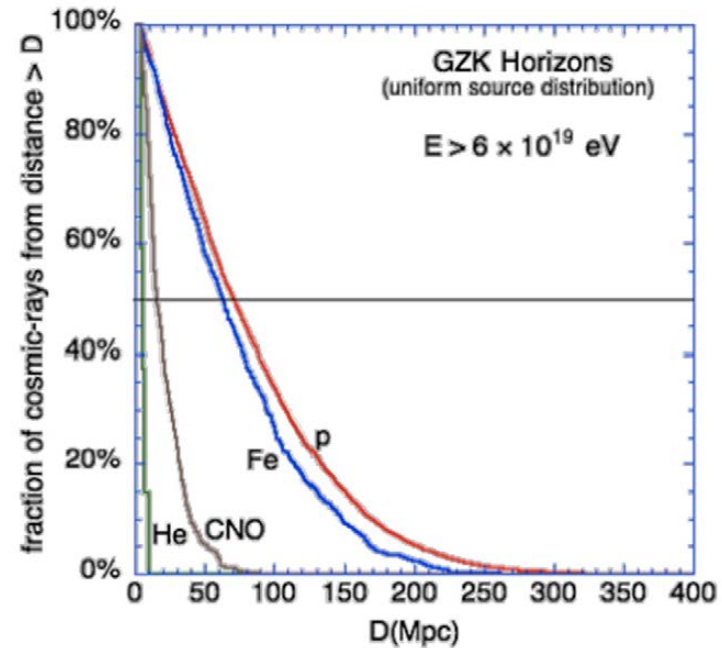
→ no excess toward the Virgo cluster?

Clues to source candidates of UHECRs



Bauleo and Martino (2009)

Hillas plot → plausible accelerators of UHECRs



Watson (2014)

GZK horizon → a substantial fraction comes from sources within 100 Mpc

Are TA hotspot events coming from a single source?

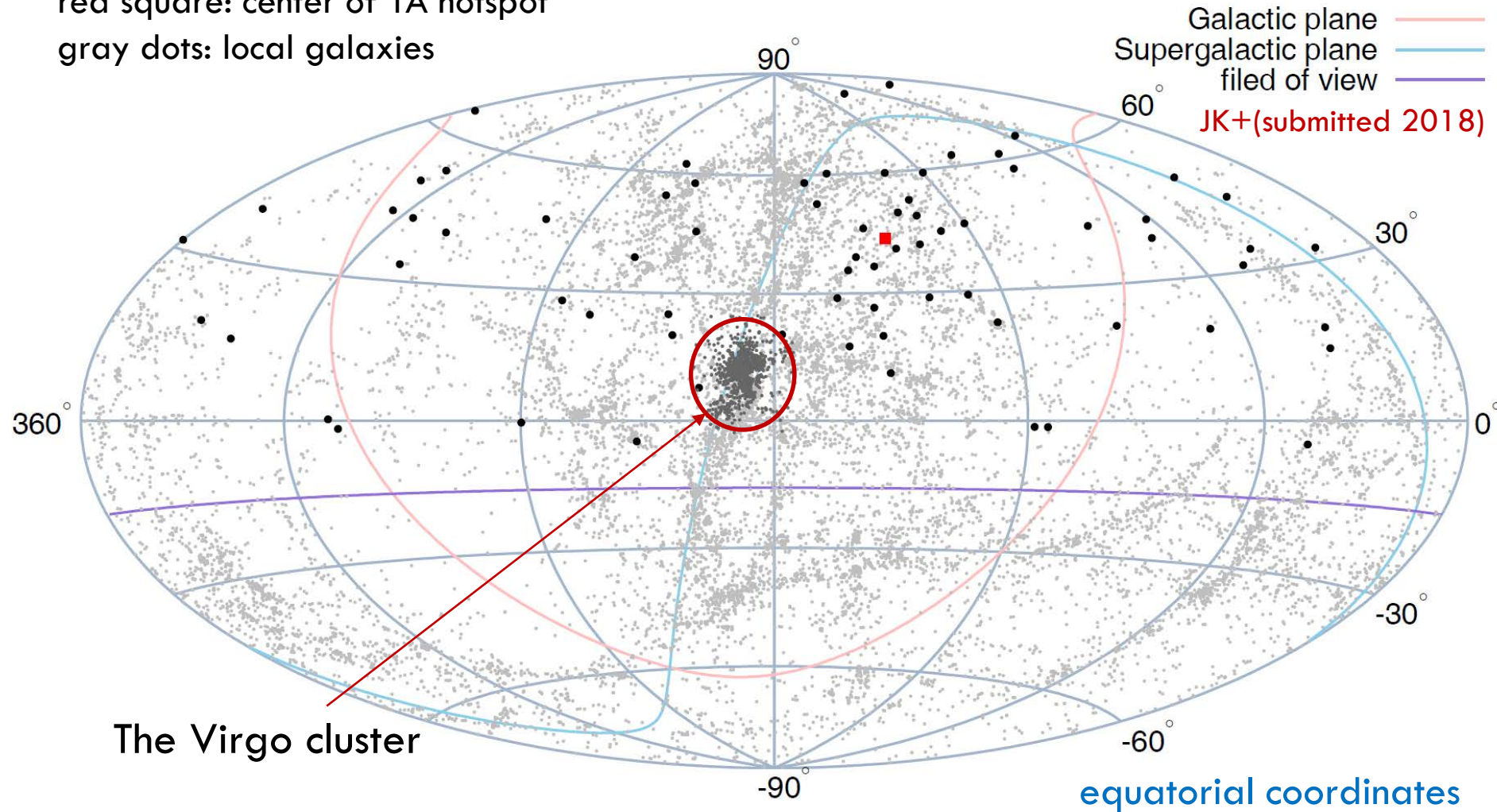
Probably not! ← No plausible nearby sources on the sky toward the TA hotspot

Search for the distribution of local galaxies

black dots: TA 5-year data TA (2014)

red square: center of TA hotspot

gray dots: local galaxies

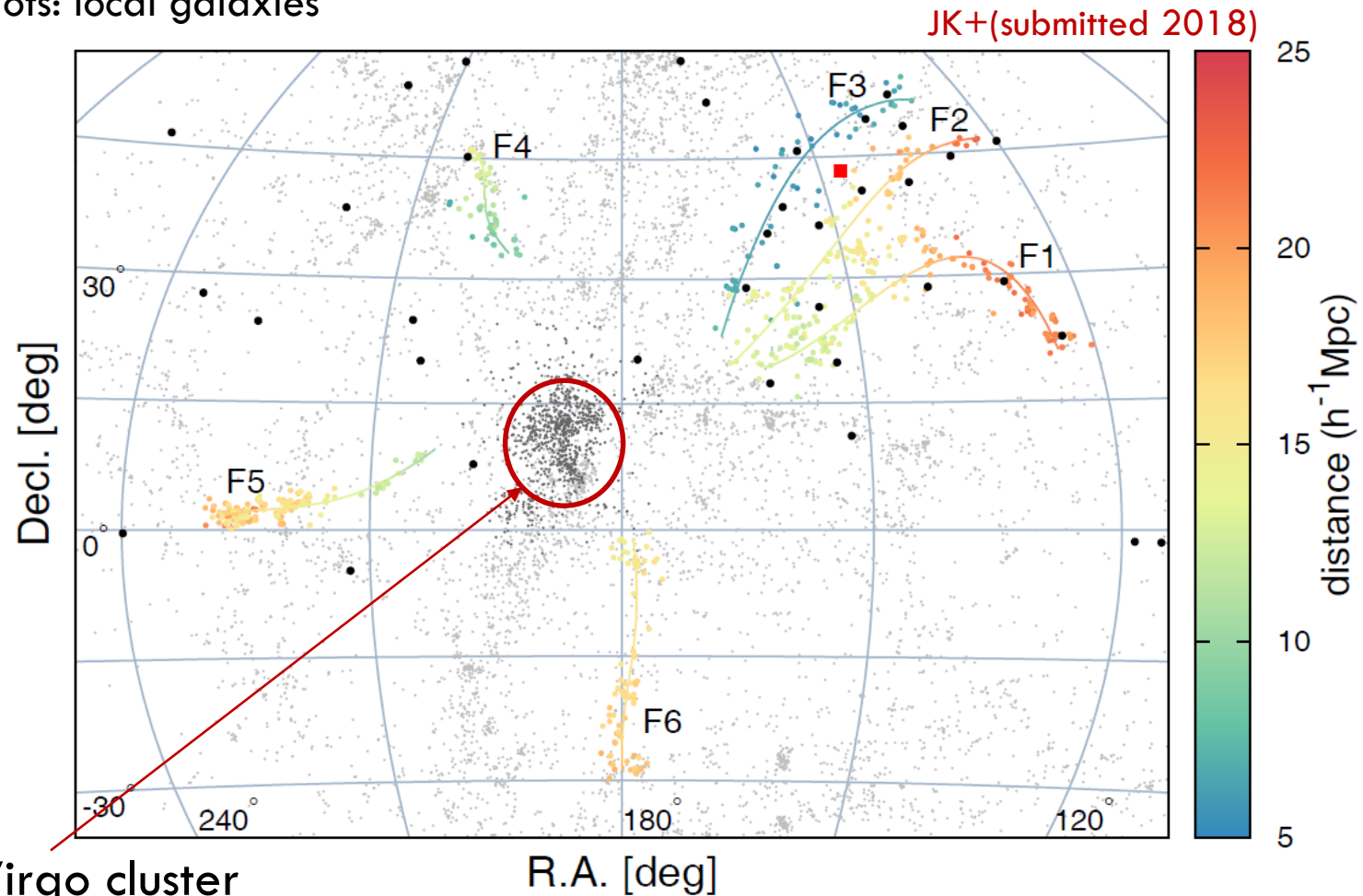


Search for the distribution of local galaxies

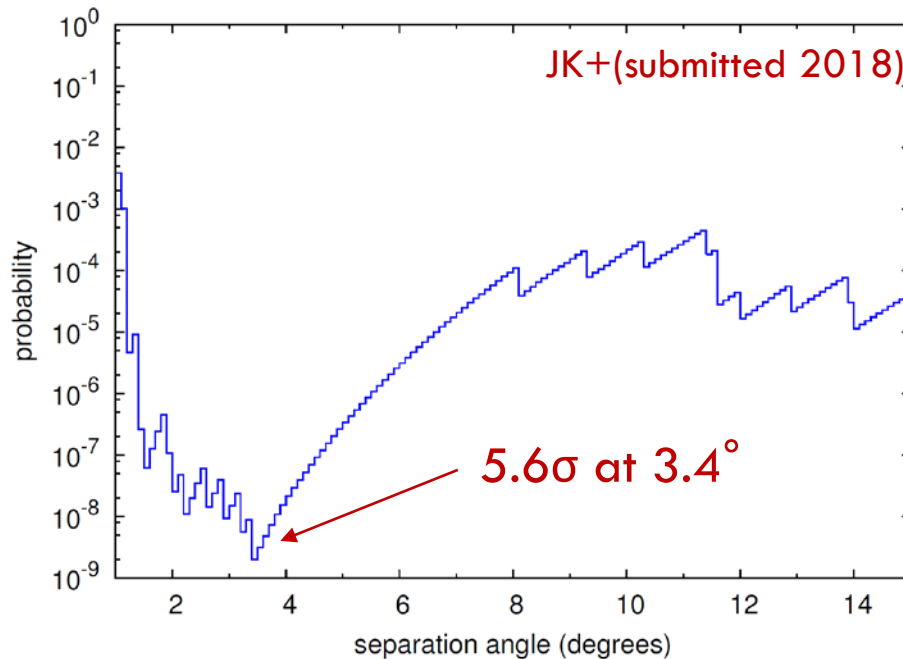
black dots: TA 5-year data TA (2014)

color dots: filaments of galaxies S. Kim et al. (2016)

gray dots: local galaxies



Summary of statistical analysis: 5-year data with 3 filaments



- 72 events with $E > 5.7 \times 10^{19}$ eV (5-year TA SD data)

- Maximum local significance: **6.1 σ**

Observed: **18** events

Expected from isotropy: **3.1** events

} **~497%** excess to the isotropy

- Post-trial probability: $P(p_{\text{pre}} > 6.1\sigma) = \mathbf{5.6\sigma}$

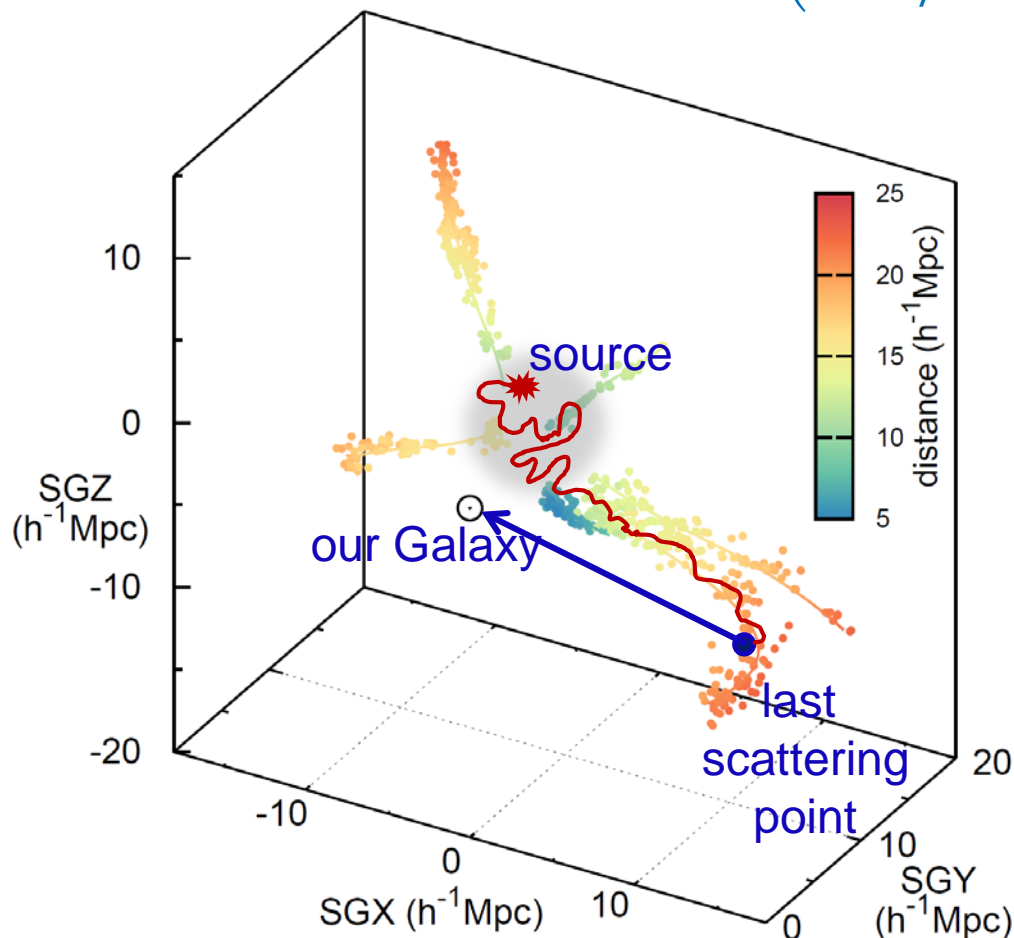
- **A close correlation** with astronomical objects with such high significance

- The estimated mass composition of UHECRs and strength of galactic magnetic fields are consistent with observations.

A plausible model for the origin of TA hotspot

JK+(submitted 2018)

$$\delta \sim f \times \frac{\pi}{2} \left(\frac{5 \times 10^{19} \text{ eV}}{E/Z} \right) \left(\frac{L}{25 \text{ Mpc}} \right)^{1/2} \left(\frac{l_c}{1 \text{ Mpc}} \right)^{1/2} \left(\frac{B_{\text{random}}}{20 \text{ nG}} \right)$$



- UHECRs are postulated to be produced at a source or sources inside the Virgo cluster. They roam around for a while because they are confined by cluster magnetic fields, and then escape through connected filaments.
- If they come to us after scattered at turbulent magnetic fields in filaments, the arrival direction of UHECRs would be correlated with the distribution of filaments on the sky.

Confinement of UHECRs

- The capability of confining a particle can be described by comparing the size of an astrophysical site, R , and the gyro-radius of the particle, r_g , which is given by

$$r_g = \frac{E}{ZeB} \sim \frac{100 \text{ kpc}}{Z} \left(\frac{E}{10^{20} \text{ eV}} \right) \left(\frac{B}{1 \mu\text{G}} \right)^{-1},$$

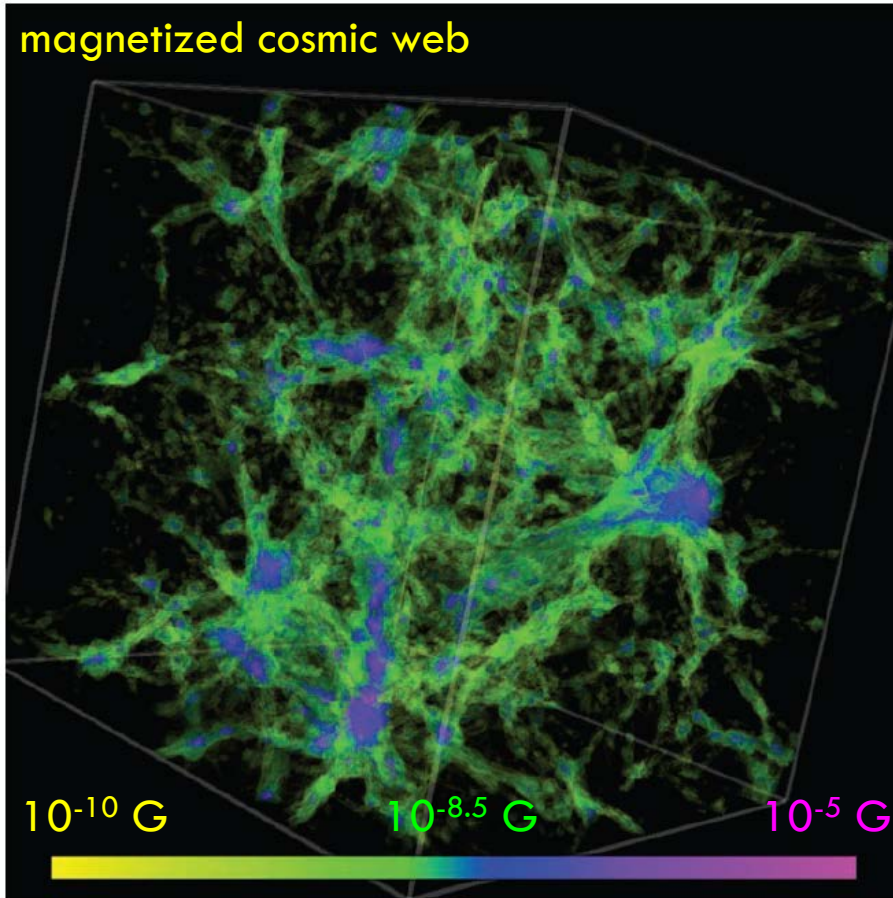
where Z and E are the charge number and energy of the particle, and B is the strength of magnetic field of an astrophysical site.

- If $R > r_g$, the particle can be confined in the astrophysical site.
- For UHECRs with $E \sim 50 \text{ EeV}$,
 - $B \sim 1 \mu\text{G} \rightarrow r_g \sim 50 \text{ kpc} \ll \text{size of galaxy clusters (several Mpc)}$
 - $B \sim 20 \text{ nG} \rightarrow r_g \sim 2.5 \text{ Mpc} \sim \text{diameter of galaxy filaments}$
- Our picture requires
 - $B > \sim 1 \mu\text{G}$ in clusters and $B > \sim 20 \text{ nG}$ in filaments

Magnetic fields in the large-scale structure from simulation

Magnetic fields in the LSS

magnetized cosmic web



Ryu et al. (2008)

- A simulated distribution of the intergalactic magnetic fields in a box of $(100 h^{-1} \text{Mpc})^3$
- Based on a turbulence dynamo model, the average strength of magnetic field would be

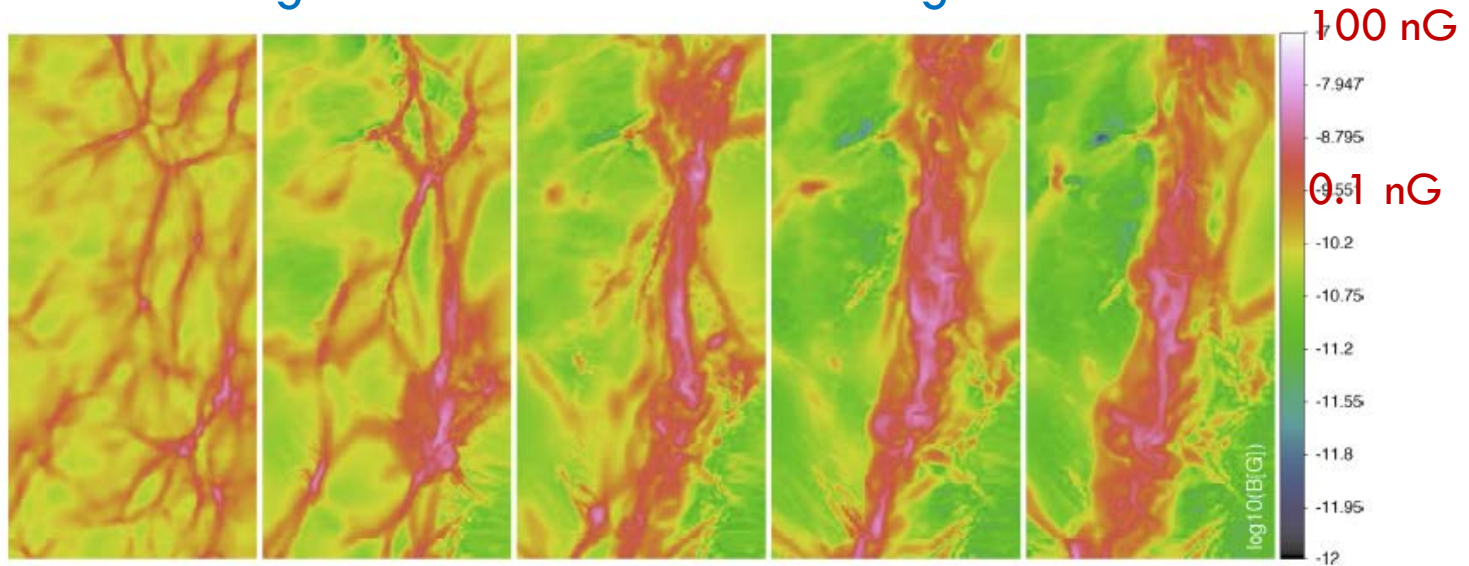
B in clusters: \sim a few μG

B in filaments: $\sim 10 \text{ nG}$

→ Consistent with the required strength of magnetic fields by our picture

Magnetic fields in the large-scale structure from simulation

Magnetic fields in filaments of galaxies



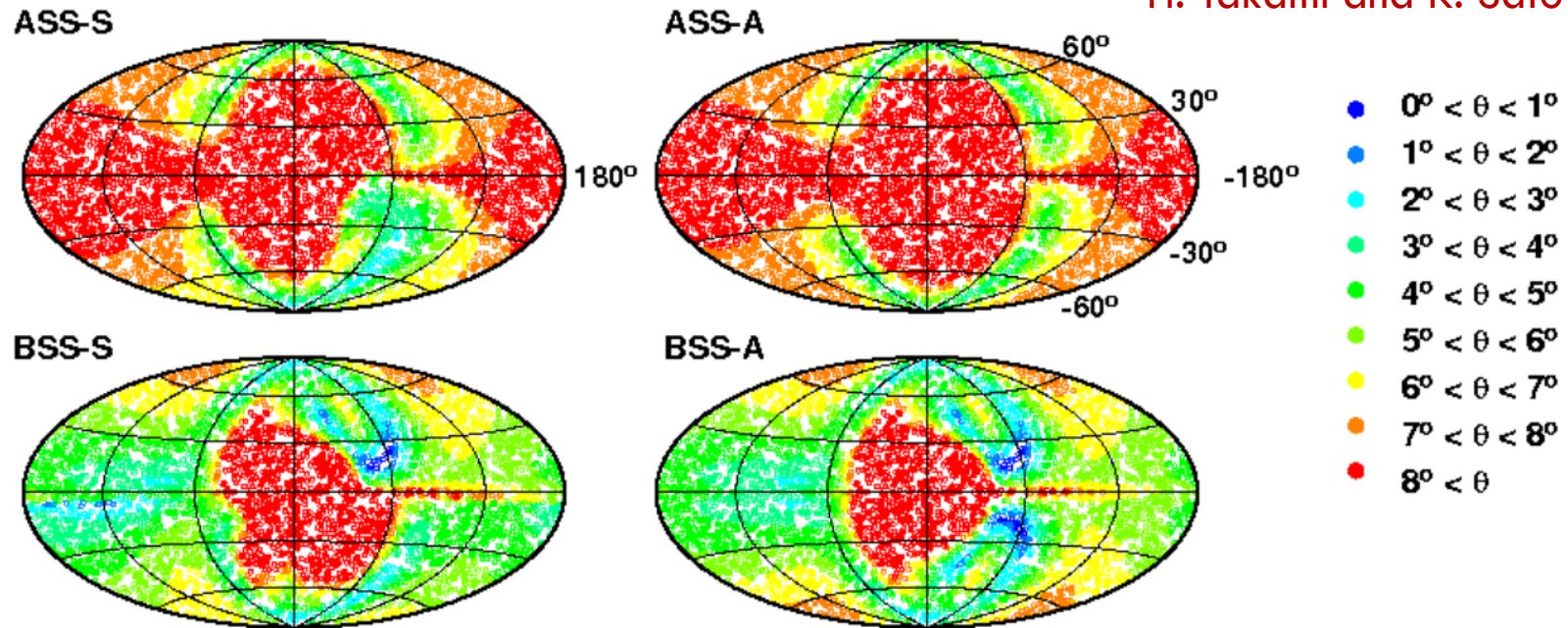
F. Vazza et al. (2014)

An evolution of magnetic fields in filaments from a simulation shown with 9 Mpc×18 Mpc image

→ Consistent with the required strength of magnetic fields by our picture

Influence by the galactic magnetic fields

H. Takami and K. Sato (2008)

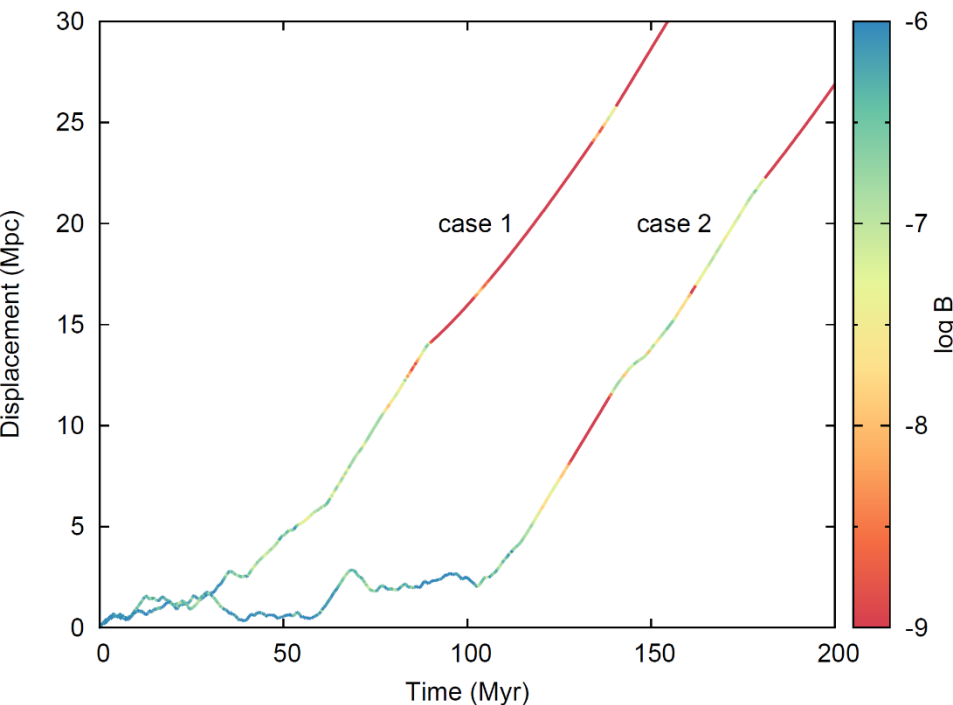


- The predicted deflection angles are highly model dependent, but it is expected that the influence of the GMF for this analysis is not too strong because the Virgo cluster and its filaments are located toward quite high galactic latitude, $> \sim 30^\circ$.

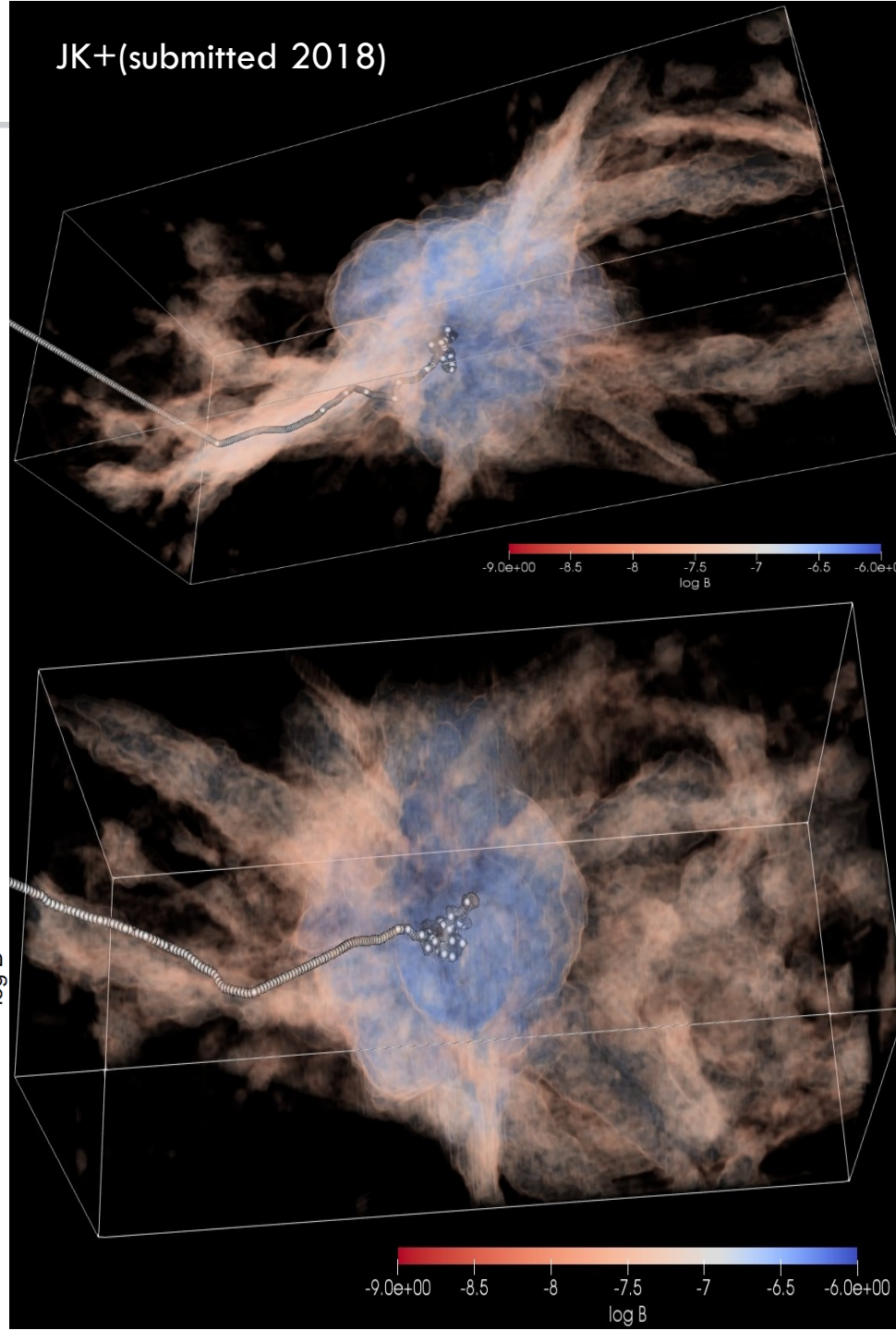
→ TA hotspot events should be light nuclei such as protons in our picture.

Trajectories of UHE protons

- UHE protons with 6×10^{19} eV
- Cluster: $T_X = 3.5$ keV
 $B_{\text{core}} \sim 1.5 \mu\text{G}$
- $42 \times 17.5 \times 17.5$ (h^{-1} Mpc)³
- UHE protons roam and escape through filaments.

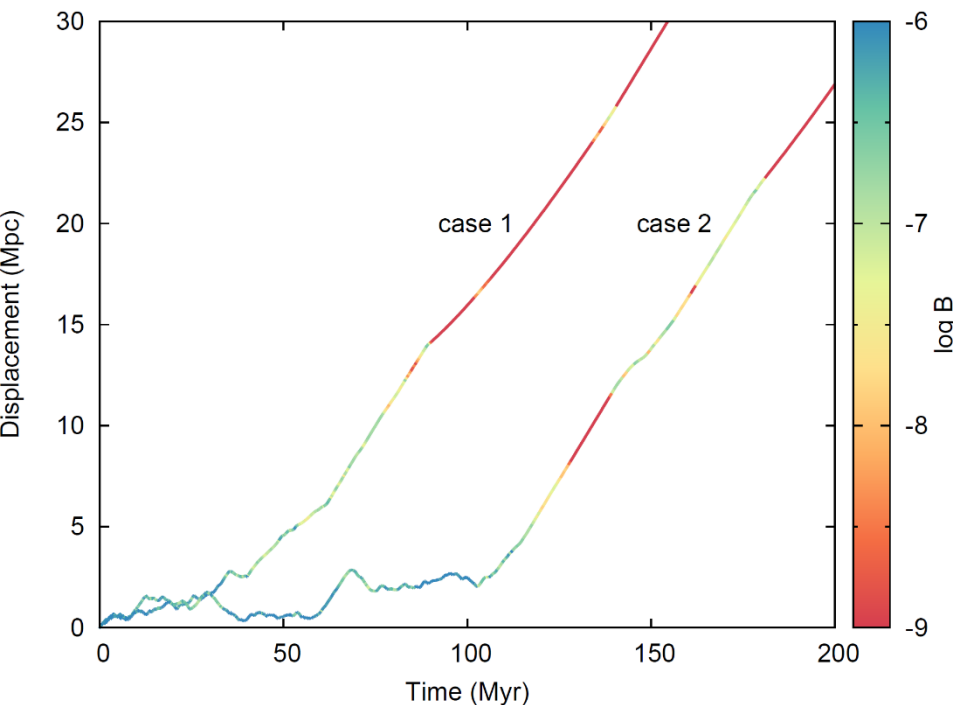


JK+(submitted 2018)

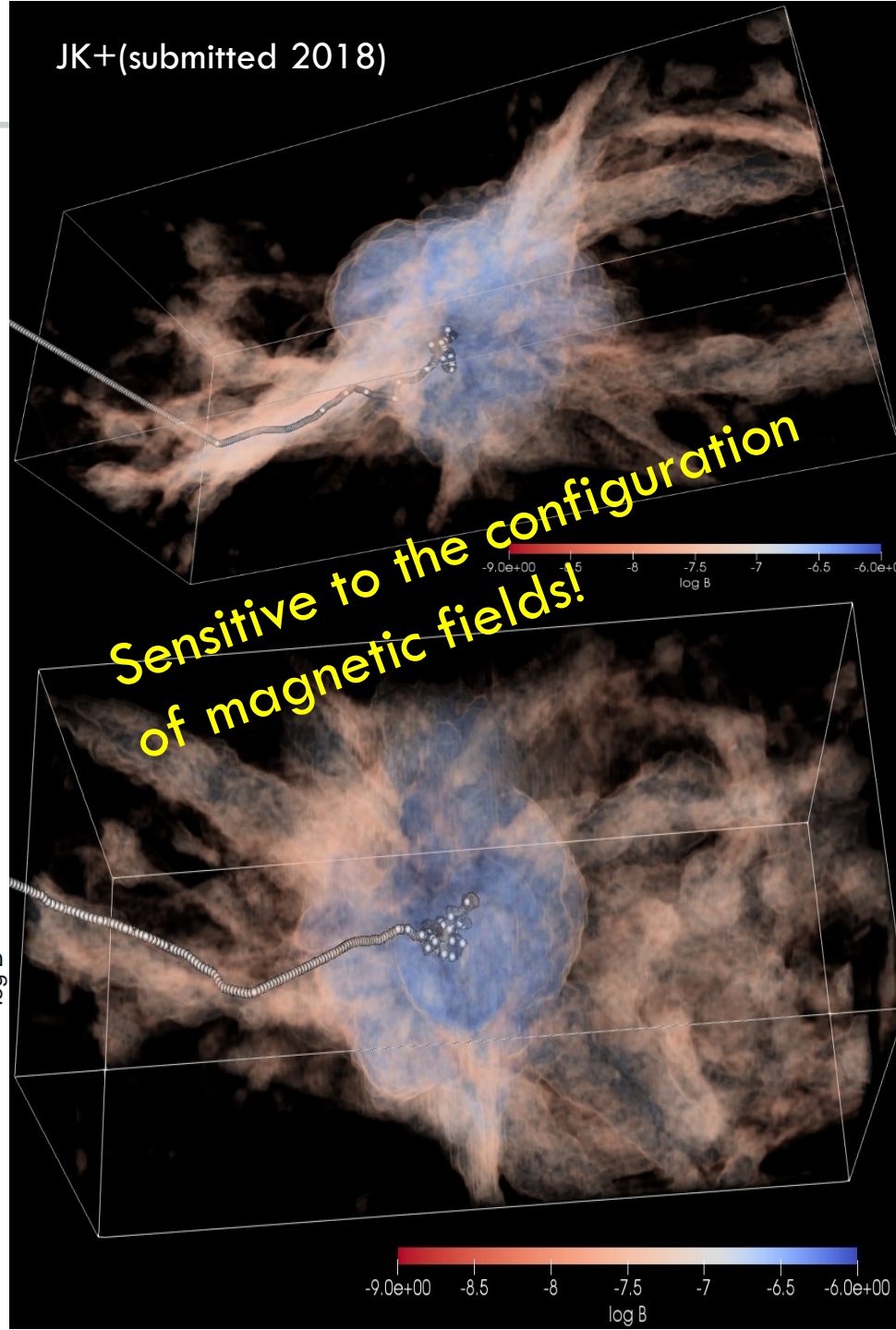


Trajectories of UHE protons

- UHE protons with 6×10^{19} eV
- Cluster: $T_X = 3.5$ keV
 $B_{\text{core}} \sim 1.5 \mu\text{G}$
- $42 \times 17.5 \times 17.5$ (h^{-1} Mpc)³
- UHE protons roam and escape through filaments.



JK+(submitted 2018)



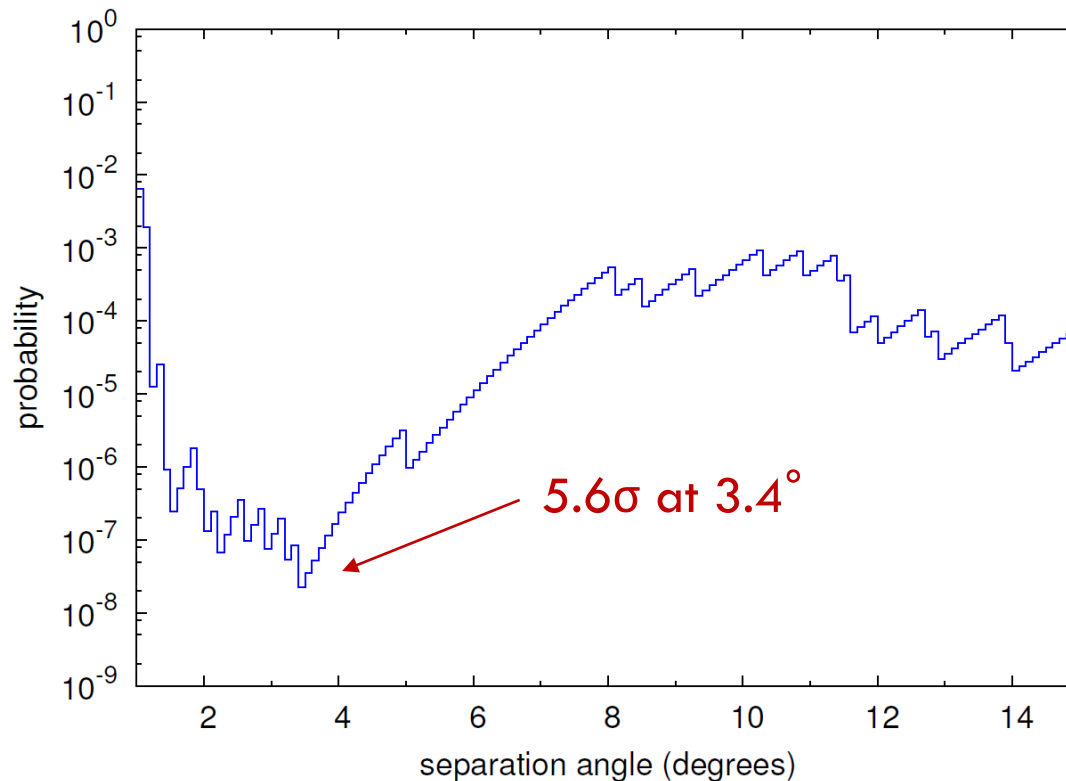
Summary

- A close correlation between the TA events and filaments of galaxies connected to the Virgo Cluster was found.
- We suggested a plausible model for the origin of TA hotspot UHECRs.
- A source (or sources) of the TA hotspot events is likely to be located in the Virgo cluster. The UHECRs would be captured by the magnetic fields in the cluster and escape toward filaments connected to the Virgo cluster, before travel to us.
- We plan to explore the dependence on the magnetic model by analyzing of various statistics in different magnetic field generation/amplification models.

Thank you.

backup

Summary of statistical analysis: 5-year data with 6 filaments



- 72 events with $E > 5.7 \times 10^{19}$ eV (5-year TA SD data)

- Maximum local significance: 5.6σ

Observed: 19 events

Expected from isotropy: 4.2 events

} $\sim 350\%$ excess to the isotropy

- Post-trial probability: $P(p_{\text{pre}} > 5.6\sigma) = 5.1\sigma$



An Indication of Anisotropy in Arrival Directions of Ultra-high-energy Cosmic Rays through Comparison to the Flux Pattern of Extragalactic Gamma-Ray Sources*

Abstract

A new analysis of the data set from the Pierre Auger Observatory provides evidence for anisotropy in the arrival directions of ultra-high-energy cosmic rays on an intermediate angular scale, which is indicative of excess arrivals from strong, nearby sources. The data consist of 5514 events above 20 EeV with zenith angles up to 80° recorded before 2017 April 30. Sky models have been created for two distinct populations of extragalactic gamma-ray emitters: active galactic nuclei from the second catalog of hard *Fermi*-LAT sources (2FHL) and starburst galaxies from a sample that was examined with *Fermi*-LAT. Flux-limited samples, which include all types of galaxies from the *Swift*-BAT and 2MASS surveys, have been investigated for comparison. The sky model of cosmic-ray density constructed using each catalog has two free parameters, the fraction of events correlating with astrophysical objects, and an angular scale characterizing the clustering of cosmic rays around extragalactic sources. A maximum-likelihood ratio test is used to evaluate the best values of these parameters and to quantify the strength of each model by contrast with isotropy. It is found that the starburst model fits the data better than the hypothesis of isotropy with a statistical significance of 4.0σ , the highest value of the test statistic being for energies above 39 EeV. The three alternative models are favored against isotropy with 2.7σ – 3.2σ significance. The origin of the indicated deviation from isotropy is examined and prospects for more sensitive future studies are discussed.

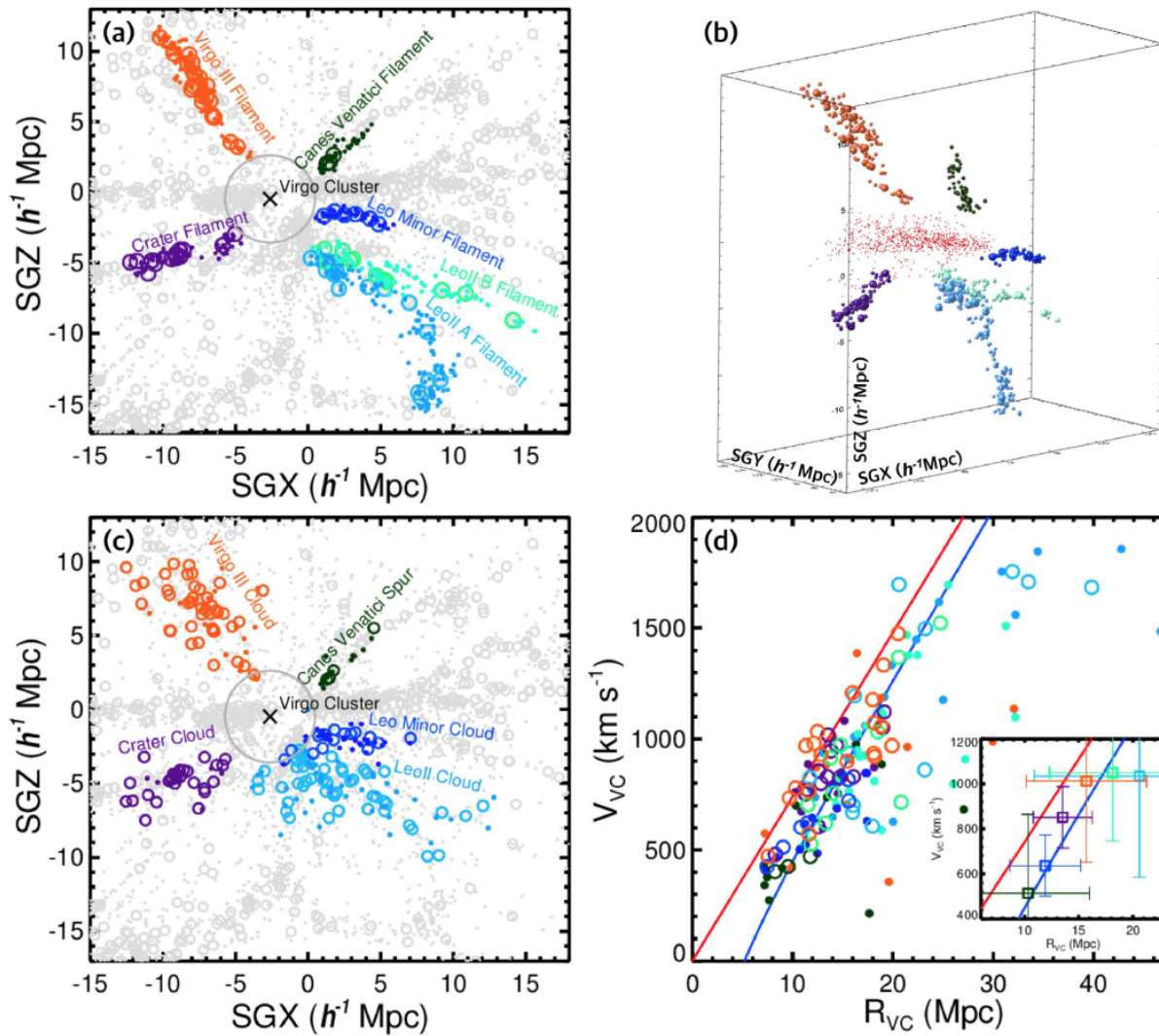
Table 2
Results—Scenario A

Test Hypothesis	Null Hypothesis	Threshold Energy ^a	TS	Local p -value $\mathcal{P}_{\chi^2}(\text{TS}, 2)$	Post-trial p -value	1-sided Significance	AGN/Other Fraction	SBG Fraction	Search Radius
SBG + ISO	ISO	39 EeV	24.9	3.8×10^{-6}	3.6×10^{-5}	4.0σ	N/A	9.7%	12.9°
γ AGN + SBG + ISO	γ AGN + ISO	39 EeV	14.7	N/A	1.3×10^{-4}	3.7σ	0.7%	8.7%	12.5°
γ AGN + ISO	ISO	60 EeV	15.2	5.1×10^{-4}	3.1×10^{-3}	2.7σ	6.7%	N/A	6.9°
γ AGN + SBG + ISO	SBG + ISO	60 EeV	3.0	N/A	0.08	1.4σ	6.8%	0.0% ^b	7.0°
<i>Swift</i> -BAT + ISO	ISO	39 EeV	18.2	1.1×10^{-4}	8.0×10^{-4}	3.2σ	6.9%	N/A	12.3°
<i>Swift</i> -BAT + SBG + ISO	<i>Swift</i> -BAT + ISO	39 EeV	7.8	N/A	5.1×10^{-3}	2.6σ	2.8%	7.1%	12.6°
2MRS + ISO	ISO	38 EeV	15.1	5.2×10^{-4}	3.3×10^{-3}	2.7σ	15.8%	N/A	13.2°
2MRS + SBG + ISO	2MRS + ISO	39 EeV	10.4	N/A	1.3×10^{-3}	3.0σ	1.1%	8.9%	12.6°

Virgo-related filaments

THE ASTROPHYSICAL JOURNAL, 833:207 (8pp), 2016 December 20

KIM ET AL.



Six filaments:
(clockwise)

Leo II minor
Leo II B
Leo II A
Crater
Virgo III
Canes Venatici

Figure 2. Spatial distribution (a)–(c) and Hubble diagram (d) of six filaments in the range $4 h^{-1} \text{ Mpc} < \text{SGY} < 16 h^{-1} \text{ Mpc}$. Symbols are the same as in Figure 1. (a) Projected spatial distribution of the filaments in the SGX–SGZ plane. The large gray circle marks two virial radii around the Virgo cluster. (b) Three-dimensional distribution of the filaments. The red dots are Virgo cluster galaxies in the EVCC. (c) Same as (a) for the structures mentioned by Tully (1982). (d) Hubble diagram of the filament galaxies in the Virgo-centric reference frame. The red and blue lines indicate the Hubble flow and a model of the radial infall velocity profile caused by the gravitational pull of the Virgo cluster, respectively. The inset shows the median Virgo-centric radial velocity and distance of each filament (error bars indicate one standard deviation).

Properties of structures

7 filaments & 1 sheet

Table 1
Filamentary Structures around the Virgo Cluster

Name	SGX (h^{-1} Mpc)	SGY (h^{-1} Mpc)	SGZ (h^{-1} Mpc)	cz (km s^{-1})	Length (h^{-1} Mpc)	R_{VC} (Mpc)	Peculiar Velocity (km s^{-1})	Distance _{MW} (Mpc)	This Work		Tully (1982)	
									N	N_{faint}	N	N_{faint}
(1)	(2)	(3)	(4)	(5)	(6)	(7)	(8)	(9)	(10)	(11)	(12)	(13)
Leo II A	0.21 ~ 10.36	9.26 ~ 15.05	-15.47 ~ -4.16	1171 ~ 2267	16.0	11.71 ~ 46.68	-213.98 (283.02)	26.30 (4.86)	180	165	97 ^b	45 ^b
Leo II B	0.30 ~ 15.65	10.90 ~ 14.56	-9.88 ~ -3.51	1257 ~ 2267	15.5	10.84 ~ 32.19	-282.04 (306.53)	26.40 (4.71)	105	94		
Leo Minor	0.55 ~ 5.89	4.11 ~ 6.49	-2.61 ~ -0.99	505 ~ 772	5.4	7.27 ~ 17.41	-250.09 (137.90)	14.07 (3.65)	54	48	46	31
Canes Venatici	0.78 ~ 4.37	6.88 ~ 13.92	1.38 ~ 4.80	674 ~ 1446	4.8	7.15 ~ 27.05	-254.95 (356.27)	20.96 (6.83)	51	48	18	14
Virgo III	-10.56 ~ -3.91	9.50 ~ 15.57	2.35 ~ 11.72	1160 ~ 2196	11.4	7.26 ~ 32.07	-102.24 (364.43)	26.70 (6.00)	181	162	61	20
Crater	-12.25 ~ -4.62	8.36 ~ 12.70	-5.91 ~ -2.98	1436 ~ 1903	7.9	8.28 ~ 19.13	-148.95 (138.52)	23.31 (3.55)	84	69	35	6
NGC 5353/4	-16.04 ~ 4.23	21.71 ~ 26.53	-1.19 ~ 8.92	2268 ~ 3238	21.9	6.70 ~ 32.27	-242.46 ^a (306.19)	41.05 (7.79)	102	89
W-M sheet	-13.38 ~ -1.66	16.03 ~ 24.99	-3.10 ~ -1.10	1806 ~ 2968	11.9	1.45 ~ 65.64	-108.85 (786.05)	32.60 (10.91)	256	221

Notes. (1) Name of the structure. (2)–(4) Range of the structure in supergalactic coordinates. (5) Range of the structure in radial velocity. (6) Length of the structure in the SGX–SGZ plane. (7) Range of the distances relative to the Virgo cluster center. (8) Median value and standard deviation of the peculiar velocities in the Virgo-centric reference frame. (9) Median value and standard deviation of the distances from the Milky Way. (10)–(11) Number of total and faint ($M_B > -19$) galaxies. (12)–(13) Number of total and faint ($M_B > -19$) galaxies in Tully (1982).

^a Median peculiar velocity and standard deviation in the NGC 5353/4 group-centric reference frame.

^b Tully (1982) designated the Leo II cloud as a single structure.

6 filaments (clockwise order)

Name	cz	(km s ⁻¹)	Length (h ⁻¹ Mpc)	R_VC	(Mpc)	Dist_MW (Mpc)	N_tot	N_faint	N_bright	N_faint/N_tot	Density_Ntot (N_tot/length)	Density_Nbright (N_bright/length)
Leo Minor	505	772	5.4	7.27	17.41	14.07	54	48	6	0.89	10.00	1.11
Leo II B	1257	2267	15.5	10.84	32.19	26.4	105	94	11	0.90	6.77	0.71
Leo II A	1171	2267	16	11.71	46.68	26.3	180	165	15	0.92	11.25	0.94
Crater	1436	1903	7.9	8.28	19.13	23.31	84	69	15	0.82	10.63	1.90
Virgo III	1160	2196	11.4	7.26	32.07	26.7	181	162	19	0.90	15.88	1.67
Canes Venatici	674	1446	4.8	7.15	27.05	20.96	51	48	3	0.94	10.63	0.63

Description for model universe

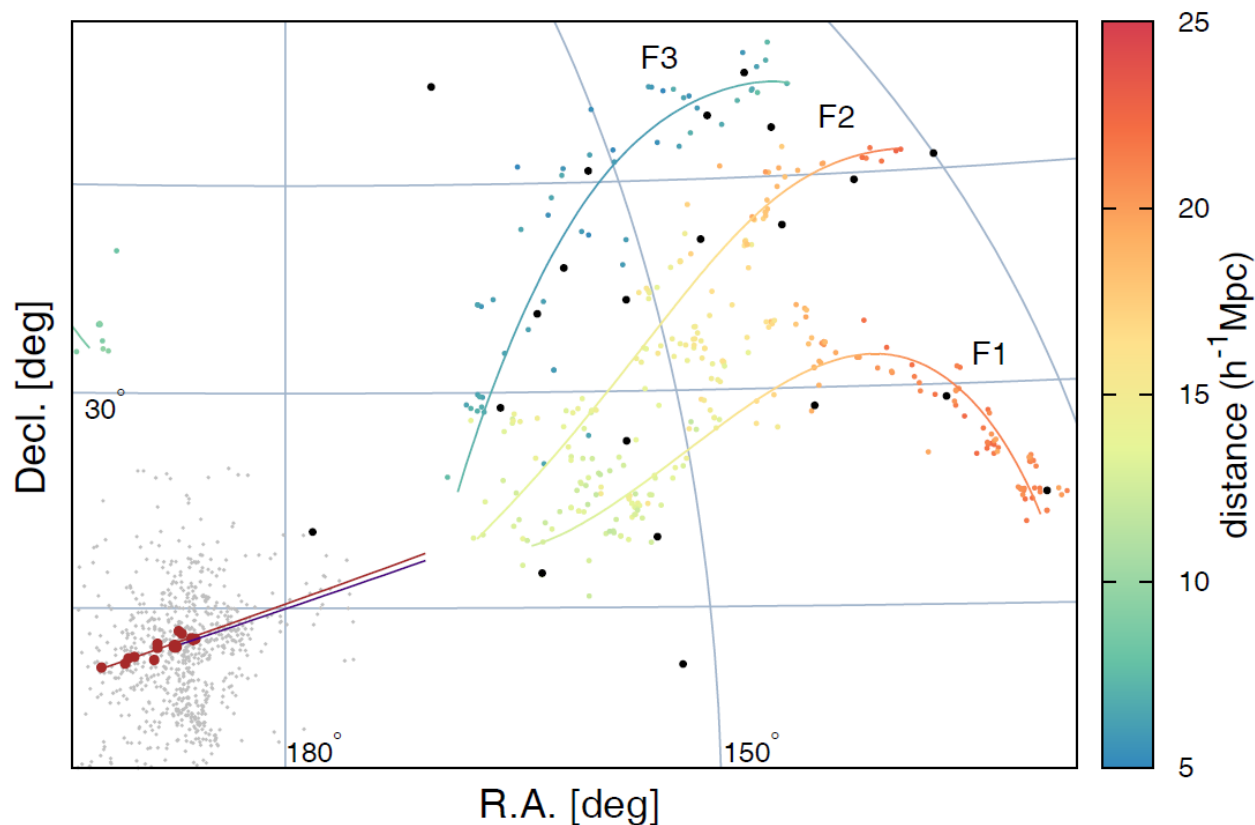
- The model universe was generated through a numerical simulation for the LSS formation using a particle-mesh/Eulerian cosmological hydrodynamics code (Ryu *et al.* 1993).
- Assuming a Λ CDM cosmological model, the following parameters were employed: $\Omega_{\text{BM}} = 0.044$, $\Omega_{\text{DM}} = 0.236$, $\Omega_{\Lambda} = 0.72$, $h \equiv H_0/(100 \text{ kms}^{-1} \text{Mpc}^{-1}) = 0.7$, $\sigma_8 = 0.82$, and $n = 0.96$.
- A cubic box of comoving size of $57 h^{-1} \text{ Mpc}$ with periodic boundaries, divided into 1650^3 uniform grid zones, was employed; the grid resolution is $34.5 h^{-1} \text{ kpc}$, which is smaller than the gyroradius of UHE protons in most zones.
- Three clusters with $T_x \gtrsim 3 \text{ keV}$ formed within the simulation volume, and a cluster with $T_x = 3.5 \text{ keV}$ was selected as the source cluster of UHE protons.

Details of simulation

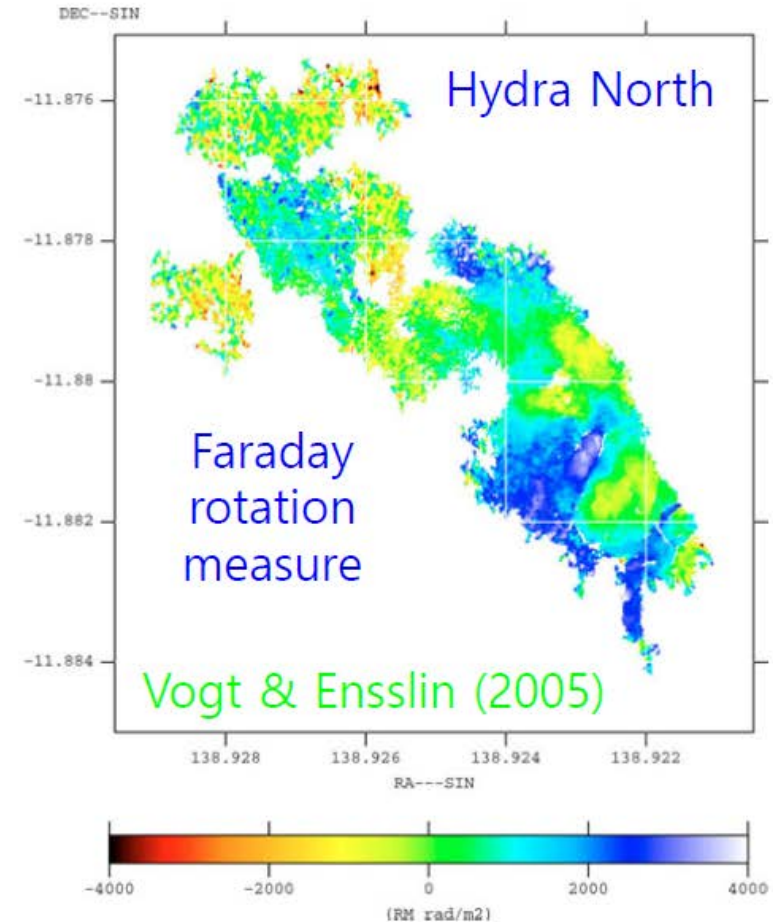
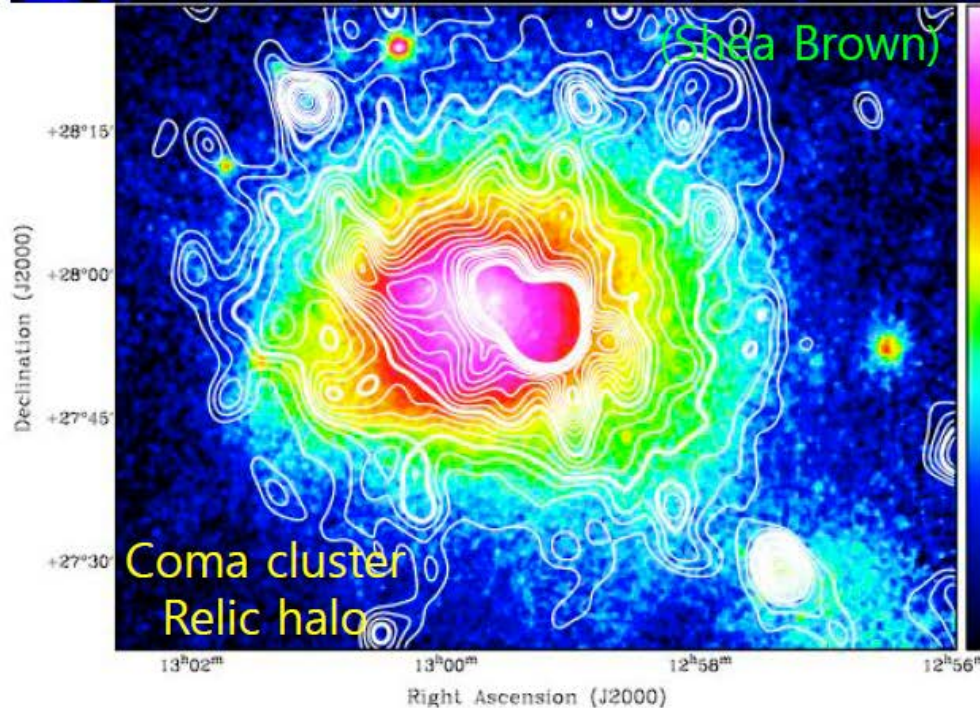
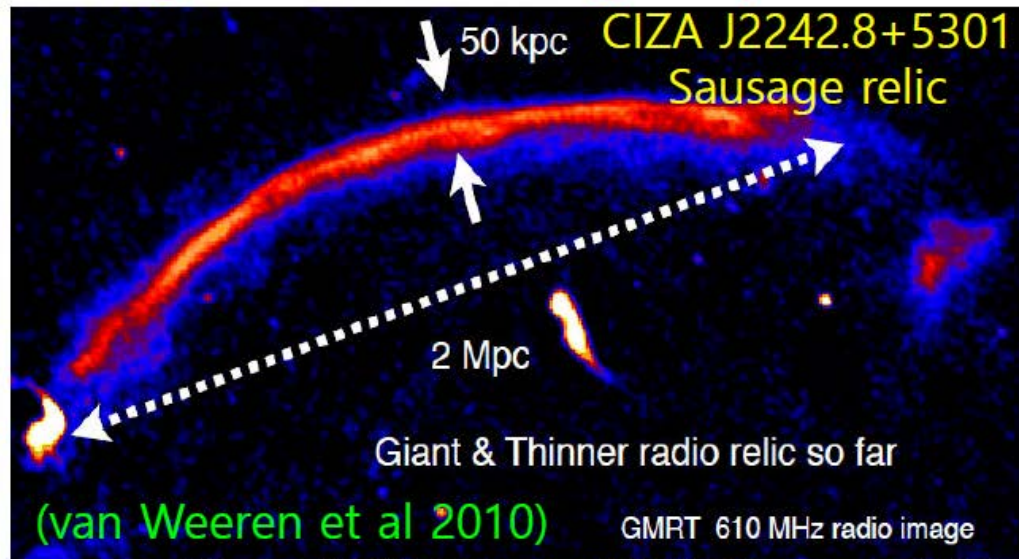
- Assuming that the intergalactic magnetic fields were seeded by the Biermann battery mechanism, their evolution and amplification were followed (Kulsrud *et al.* 1997).
- However, with the numerical resolution employed, the cluster magnetic fields are not amplified to the level of observed strengths (Vazza *et al.* 2017). Therefore, the magnetic field strength in the core (within $1 h^{-1}$ Mpc from the X-ray center) of the source cluster was rescaled to $\sim 1 \mu\text{G}$; then it became $\sim 0.1 \mu\text{G}$ in the cluster outskirts, and a few tens of nG in filaments.
- At random positions within the cluster core, UHECRs with 6×10^{19} eV were injected toward random directions, and their trajectories were followed with the relativistic equation of motions for charged particles under magnetic field.

Intriguing observations in the Virgo cluster

- Brown circles and the brown line plot brightest elliptical galaxies and the extension of the cluster principal axis, respectively, in the Virgo Cluster. The extension of M87 jet is drawn with the indigo line.



Magnetic fields in galaxy clusters appears in observations



D. Ryu@UHECR2016

Clusters of galaxies – numbers and energetics

density of baryonic matter

$$n \sim 10^{-2} \text{ cm}^{-3}$$

flow velocity

$$v \sim \text{several} \times 10^2 \text{ km/s}$$

gas temperature

$$T \sim 10^8 \text{ K}$$

magnetic fields

$$B \sim \text{a few } \mu\text{G}$$

gas kinetic energy

$$E_{\text{kinetic}} \sim 10^{-11} \text{ erg/cm}^3$$

gas thermal energy

$$E_{\text{thermal}} \sim 10^{-10} \text{ erg/cm}^3$$

magnetic energy

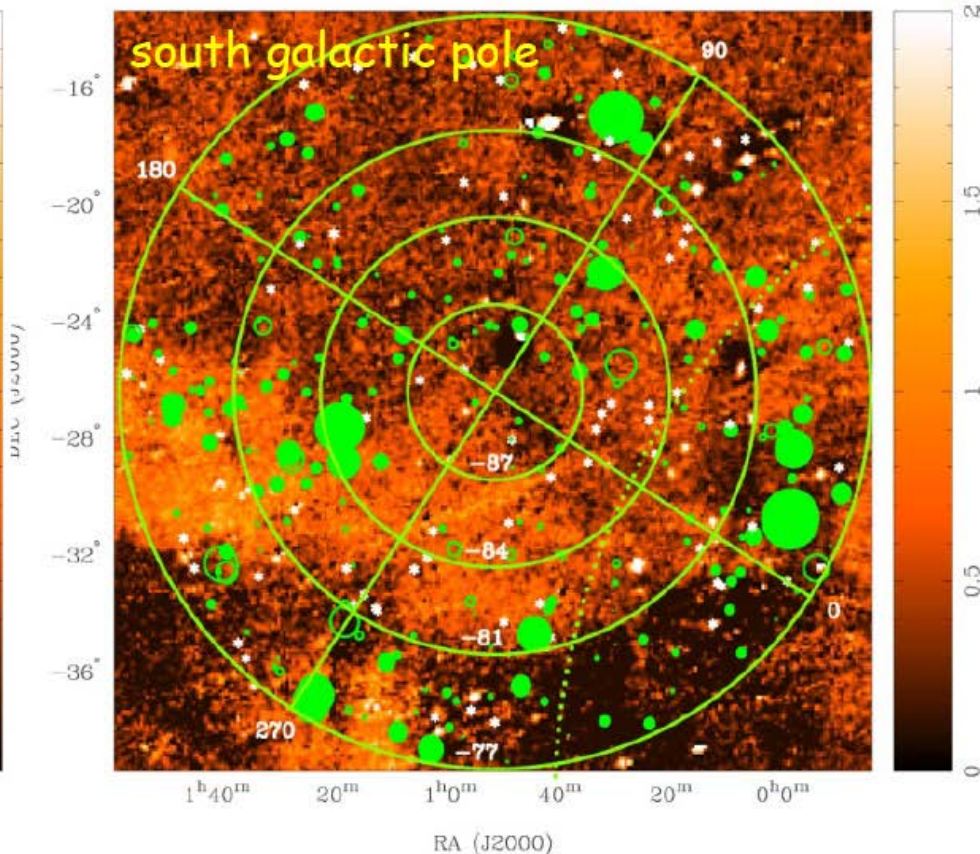
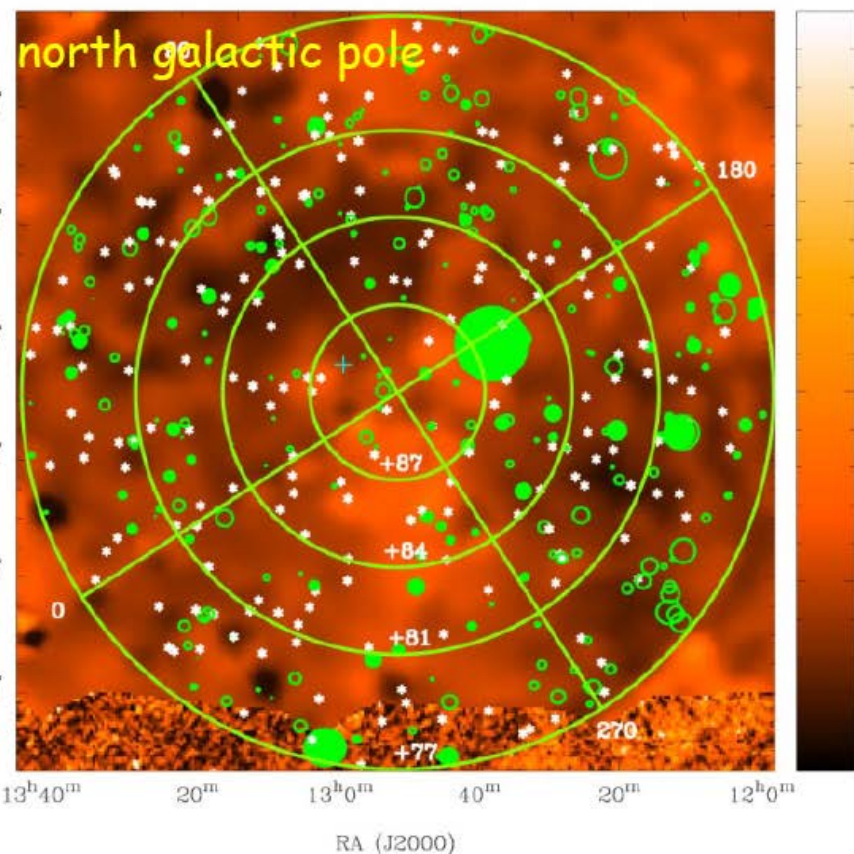
$$E_{\text{magnetic}} \sim 10^{-12} \text{ erg/cm}^3$$

D. Ryu@UHECR2016

Magnetic fields in filaments of galaxies

faraday rotation measure

Mao et al (2010), Stil et al (2011)



→ extragalactic contribution of $\sim 6 \text{ rad/m}^2$

Schnitzeler et al (2010)

mostly due to magnetic fields in filaments of galaxies

→ $B \sim 10 \text{ nG}$ (needs to be further confirmed) D. Ryu@UHECR2016

Filaments of galaxies – numbers and energetics

density of baryonic matter

$$n \sim 10^{-5} \text{ cm}^{-3}$$

flow velocity

$$v \sim \text{a few} \times 10^2 \text{ km/s}$$

gas temperature

$$T \sim 10^6 \text{ K}$$

magnetic fields

$$B \sim 10 \text{ nG}$$

gas kinetic energy

$$E_{\text{kinetic}} \sim 10^{-14} \text{ erg/cm}^3$$

gas thermal energy

$$E_{\text{thermal}} \sim 10^{-15} \text{ erg/cm}^3$$

magnetic energy

$$E_{\text{magnetic}} \sim 10^{-17} \text{ erg/cm}^3$$

D. Ryu@UHECR2016

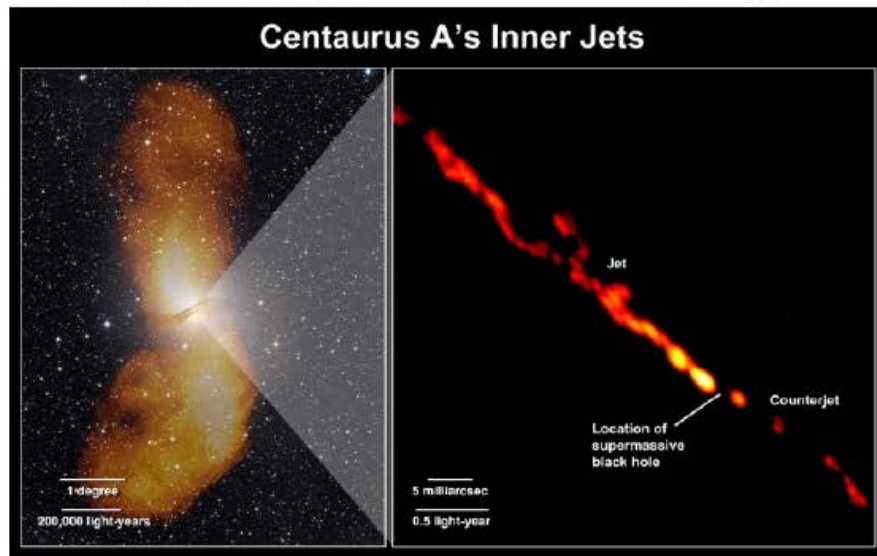
Virgo A, a radio galaxy, as sources of UHECRs ?

shock acceleration or
turbulent acceleration

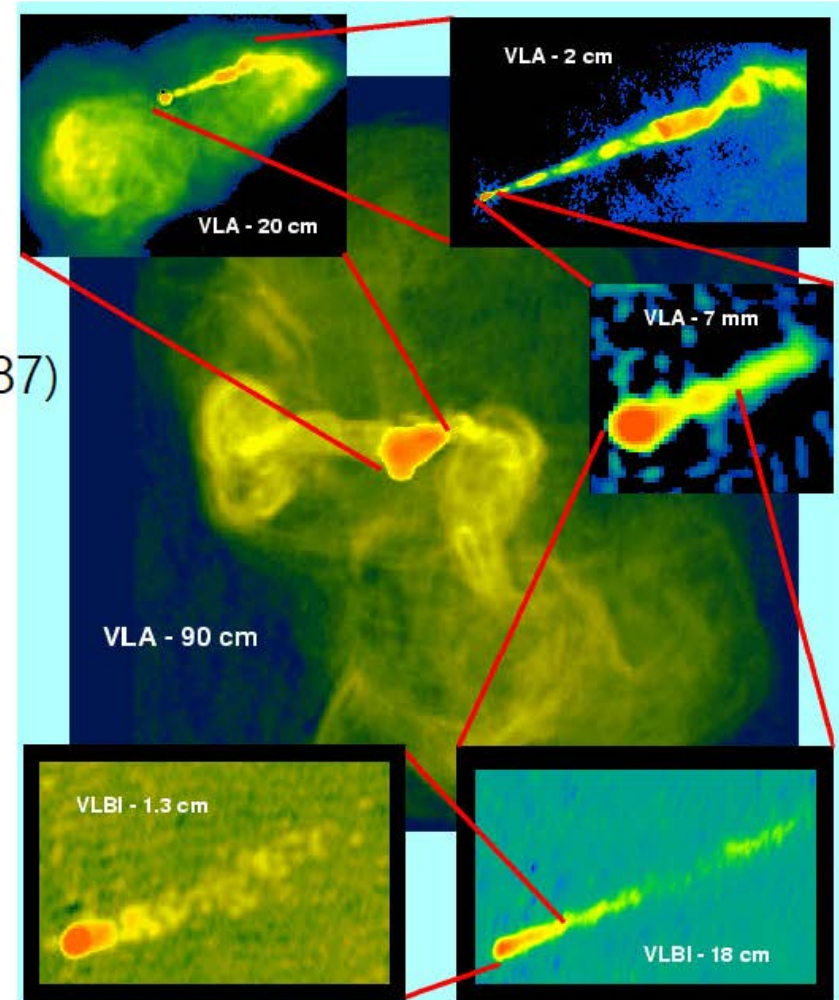
→ OK for Fe, not for p ?

Centaurus A

Virgo A (M87)



Properties of the FR I radio galaxies Cen A, M 87 and Fornax A.



source	size (kpc)	d (Mpc)	L_{radio} (erg s ⁻¹)	M_{BH} (M_{\odot})	L_j (erg s ⁻¹)	θ (°)	V_{GL} (pc ⁻³)	B_{GL} (μG)
Cen A	600	3.8		$5.5 \cdot 10^7$	$1 \cdot 10^{43}$	50		0.9
M 87	70	16.7		$3.2 \cdot 10^9$	$4 \cdot 10^{44}$	15 - 25		7.0
Fornax A	290	18.6		$1.5 \cdot 10^8$				1.5

D. Ryu@UHECR2016